Enhancement of thermal and electrical properties of carbon nanotube polymer composites by magnetic field processing

E. S. Choi,[a] J. S. Brooks, and D. L. Eaton
NHMFL, Florida State University, Tallahassee, Florida 32310

M. S. Al-Haik and M. Y. Hussaini
Department of Mechanical Engineering, Florida State University, Tallahassee, Florida 32310

H. Garmestani and D. Li
Materials Science and Engineering, Georgia Institute of Technology, Atlanta, Georgia 30332

K. Dahmen
Department of Chemistry, Florida State University, Tallahassee, Florida 32306

(Received 8 May 2003; accepted 18 August 2003)

We show that the thermal and electrical properties of single wall carbon nanotube (CNT)-polymer composites are significantly enhanced by magnetic alignment during processing. The electrical transport properties of the composites are mainly governed by the hopping conduction with localization lengths comparable to bundle diameters. The bundling of nanotubes during the composite processing is an important factor for electrical, and in particular, for thermal transport properties. Better CNT isolation will be needed to reach the theoretical thermal conductivity limit for CNT composites. © *2003 American Institute of Physics.* [DOI: 10.1063/1.1616638]

I. INTRODUCTION

The addition of small quantities of carbon nanotubes (CNTs) to polymer composites is known to cause a dramatic increase in the thermal conductivity of the polymer host.[1] The thermal conductivity will change from around 0.1 to 1 W/mK for neat polymers, to as much as 10 W/mK for single-wall carbon nanotube (SWNT) composites. Presently, the thermal conductivity for an isolated multiwall carbon nanotubes (MWNTs) is estimated at 3000 W/mK (Ref. 2) and 1750–5800 W/mK for SWNTs,[3] which may be taken as the upper limit of thermal conductance in a composite material (assuming a linear law of mixing, and nanotube–polymer interactions notwithstanding). The properties of noncomposite CNT assemblies may be further enhanced by magnetic alignment.[4,5] However, the theoretical limit to such assemblies is the thermal crosslinking between connected nanotubes which diffuses the thermal wave vector k.[6] Hence, the goal of the present work has been to (1) separate the nanotubes by interaction with polymers to reduce Δk, and (2) employ the advantage of magnetic alignment to enhance the colinearity of k for each nanotube in the composite.

The alignment of CNTs in magnetic fields arises from the anisotropic magnetic susceptibility of nanotubes.[7] Walters *et al.*[8] demonstrated alignment of SWNTs by filtering the SWNT suspension in the high magnetic field.[8] The low viscosity of SWNT suspension in dimethylformamide made it possible for the SWNT to reorient parallel to the magnetic field, overcoming the Brownian motion. A host material with rather high viscosity (0.1–0.9 Ns/m^2) was also used to make a MWNT–polymer composite, where a mixture of MWNT and unsaturated polyester was placed in a 10 T magnet, followed by the polymerization of the composites to freeze the alignment.[9] In the case of high viscosity polymeric hosts, the alignment is a cooperative process involving the anisotropic magnetic susceptibility of both the CNT and polymer systems. The anisotropy of the MWNT polymer in Ref. 9 was verified by transmission electron microscopy (TEM), electrical, magnetic, and mechanical property measurements. In the work reported here for SWNTs, the magnetic field alignment also involves a high viscosity polymeric host, and cooperative effects are evident. The reorientation of the SWNT is related to the self-organizing process of the polymeric system, that is, a stretching effect that the magnetic field exerts on the crosslinked epoxy network. Here, we focus on the dependence of the electrical and thermal transport properties of this material versus magnetic field value during processing, and for different transport directions with respect to processing field orientation.

The electrical conductivity is a sensitive probe of composites. Indeed, the percolation behavior in the electrical conductivity of nanotube–polymer composites has been widely studied for several years. The high aspect ratio of CNTs is known to be advantageous in making a percolation network at relatively small loading percentages (of order 1 wt %) of nanotubes. Relevant to the present work is the advantage that the intrinsic electrical conduction processes of nanotubes, such as localization and Coulomb correlation, can be studied in nanotube–polymer composite materials.[10] We have performed both electrical and thermal conductivity measurements on SWNT–epoxy composite materials prepared with various magnetic processing conditions. We find that the electrical and thermal properties are enhanced for the magnetically aligned nanotube composites. From the temperature and electric-field dependence of electrical conductivity, we determine that the localization length in the hop-

[a]Electronic mail: echoi@magnet.fsu.edu

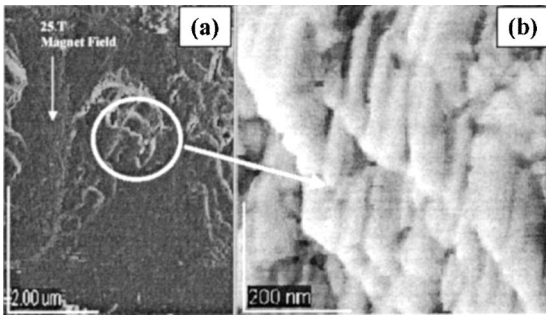

FIG. 1. Atomic force microscopy for a SWNT–epoxy composite processed in a 25 T magnetic field. The image on the right-hand side (b) represents the enhanced detail of the encircled area in the image on the left-hand side (a). The lighter structures are bundles of aligned nanotubes of about 20 to 30 nm in diameter and of order 200 nm in length.

ping conduction regime increases by magnetic alignment. We also discuss the effect of alignment in the magnetic processing, that may, based on the analysis of the electrical transport data, cause enhanced dispersion and bundling of nanotubes in the epoxy matrix.

II. EXPERIMENTAL PROCEDURES

A. Materials and magnetic field processing

Purified SWNTs from Carbon Nanotechnologies[11] were dispersed ultrasonically with a small amount of ethanol in an ultrasonic bath at room temperature for 30 min. After mixing the ethanol-based solution into the Thixotropic/PR2032 epoxy resin,[12] a similar amount of ethanol was added and the whole mixture was ultrasonicated for 30 min. This process promoted the distribution of carbon nanotubes over the surface of the resin, and prevented particle clustering. After mixing the ethanol-based solution into the resin, the suspensions were stirred for 15 min at 2000 rpm. During the stirring process, the temperature of the resin was kept at 25 °C in a cold water bath to maintain the low viscosity of the resin. In order to evaporate the ethanol, the mixture was placed in an ultrasonic hot water bath at 50 °C for another 30 min. After adding the PH3660 hardener, the mixture was stirred mechanically for 5 min. The resin/hardener mix ratio for each sample was 4:1 weight with an uncured density of 1110 kg/m^3 and viscosity of 0.90–0.95 Ns/m^2.[12] The epoxy/nanotube system had 3% nanotubes by weight. The liquid systems were degassed in a moderate vacuum until all gas bubbles disappeared, and then injected separately, using 10 mm syringes, inside quartz tubes of 8 mm in diameter and 50 mm long. The quartz tubes were sealed and taped vertically to a cylindrical sample holder, which was then positioned at the center of the high-field magnet.

Samples of neat epoxy and compositions of epoxy +3 wt % SWNT were processed in magnetic fields of 0, 15, and 25 T. The magnetic alignment sequence involved 2 h at room temperature, followed by 2 h at 60 °C, where the magnetic field was held constant for the entire 4 h period. An example of a magnetically processed (25 T) SWNT–epoxy composite structure is shown in the atomic force microscope (AFM) picture in Fig. 1. As discussed above, it is believed that the reorientation of CNTs in a polymeric medium occurs due to the cooperative effect of the magnetic torque exerted by the magnetic field directly on the nanotubes and by the hydrodynamic torque and viscous shear (i.e., drag forces) exerted on the nanotubes by the polymer chains, which also respond to the field due to magnetic anisotropy. (The sample morphologies for different magnetic process conditions have been studied in detail by electron scanning environmental microscopy, atomic force microscopy, and wide-angle x-ray diffraction, and will be reported elsewhere.)[13]

B. Electrical and thermal transport measurements

For the electrical resistance measurements, the samples were cut into thin square slabs with typical dimensions of $3\times3\times0.6$ mm^3. The volume resistivity was measured using a high input impedance electrometer (Keithley 6517A, Cleveland, Ohio) by a voltage bias across the thickest direction, and measuring the current. The electrical contact was made using a silver paste with a ring guard electrode configuration to reduce any effect of leakage currents. Since large voltages were used (typically 100 V) to maintain good signal to noise, we checked for possible heating effects by varying the voltage biasing conditions. When voltage bias pulses with different widths (0.1–30 s) were applied, no recognizable time dependence in the value of the resistance was observed. Other contact methods, such as pressure contacts with an indium foil as a binding material, showed large time dependent hysteresis effects in current–voltage ($I-V$) measurements, and were not used in our study.

For thermal conductivity measurements, the comparative method was used with constantan wire as a reference material, and miniature thermocouples were used as temperature sensors. A sample was cut into a long bar shape with typical dimensions $5\times0.2\times0.2$ mm^3 and attached to a constantan wire which is thermally connected to a heater. By comparing the temperature difference across the sample and constantan wire, the relative thermal conductivity of the sample to the constantan wire was obtained. In all cases, the samples were measured in a diffusion-pumped vacuum to eliminate shorting of conducting paths by air or condensation.

III. RESULTS

A. Electrical transport

The temperature dependence of resistivity $[\rho(T)]$ of control epoxy (E-25T: cured at 25 T without CNTs) and CNT–epoxy composites are presented in Fig. 2. Hereafter, we denote CNT–epoxy composites as CE-0T for a composite without a magnetic process, CE-15T for a composite cured at 15 T, and CE-25T for a composite cured at 25 T. CE-15T samples were cut into two different pieces so that applied voltage is either parallel (CE-15T$_\parallel$) or perpendicular (CE-15T$_\perp$) to the nanotube alignment direction. In some cases, different samples with same magnetic process conditions were measured and are denoted as, e.g., CE-15T$_\perp$A or CE-15T$_\perp$B. The room-temperature resistivity decreases by six orders of magnitudes by loading 3 wt % of SWNTs. The resistivity decreases further by magnetic alignment. For instance, the resistivity of CE-25T$_\parallel$ decreased by 35% of CE-0T at room temperature. Anisotropy is also observed be-

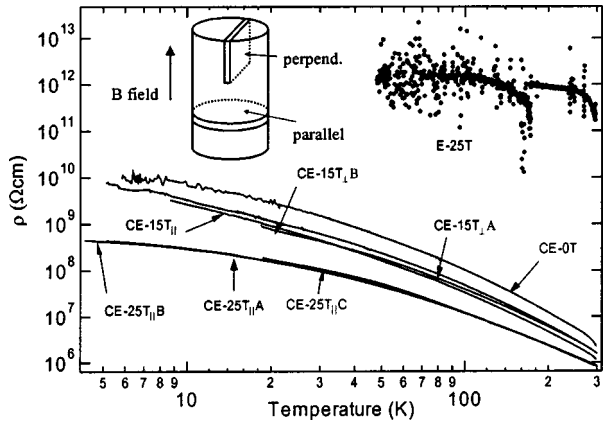

FIG. 2. Temperature dependence of resistivity of magnetically processed CNT–epoxy composites. The current was applied along the thickest direction of a slab- or disk-shaped sample, as cut from the magnetically processed cylindrical sample shown in the inset. (The resistivity of the neat epoxy was near the limit of the ability of the instrumentation to maintain ohmic behavior.)

tween the CE-15T$_{\parallel}$ and CE-15T$_{\perp}$ samples with ρ(CE-15T$_{\perp}$)/ρ(CE-15T$_{\parallel}$)$\sim$1.4 at room temperature. The temperature dependence of the anisotropy is very weak; and at a lower temperature, the anisotropy increases slightly, showing a maximum of 1.5 at 60 K and decreases to 1.2 at 8 K.

Since the nanotube–epoxy composite materials are moderately high in resistivity, and disorder-related transport mechanisms are evident, we also investigated the nonlinear electric field effects, as shown in Fig. 3. For the temperature dependent measurement, an independently cut CE-25T$_{\parallel}$ sample (hereafter CE-25T$_{\parallel}$B) was used. The nonlinearity of resistance is significant for all samples, which is typical in a hopping conduction system.

1. Theoretical analysis of electrical transport in composites

The results of the temperature and electric-field dependent resistivity measurements yield important microscopic information about these materials. In this section, we consider the mechanisms for the electrical transport characteristics discussed above and presented in Figs. 2 and 3. Electrical conduction of nanotube mat or nanotube composites is often explained by a variable range hopping (VRH) conduction model.[11,14–16] The temperature dependence for the VRH conduction can be expressed as

$$\rho(T)=\rho_0 \exp\left(\frac{T_m}{T}\right)^m, \tag{1}$$

where $m=1/4$ for the three-dimensional (3D) Mott VRH model.[17] For the Efros VRH model, where the Coulomb interaction is important, the exponent m is 1/2.[18] For both Efros and Mott VRH models, the numerator in the exponent, T_m, is related to a localization length (ξ) as

$$T_{1/2}=\frac{\beta_{1/2}e^2}{k_B\kappa(\xi)\xi} \quad \text{for the Efros VRH,}$$

$$T_{1/4}=\frac{\beta_{1/4}}{k_B n(E_F)\xi^3} \quad \text{for the Mott VRH model,} \tag{2}$$

where β's are constants, κ is the dielectric constant, and $n(E_F)$ is the density of states at the Fermi level.

In the hopping conduction regime, the resistance is dependent on electric field, due to either electric field effects, or to hot electron effects. In the field effect model, the electric field is assumed to assist tunneling between localized states, so that the resultant resistivity can be expressed as

$$\rho(T,E)=\rho(T)\rho(E)=\rho_0 \exp\left(\frac{T_m}{T}\right)^m \exp\left(-\frac{cE\lambda}{kT}\right), \tag{3}$$

where λ is a characteristic hopping length.[19] In the hot electron model, the effect of the electric field is to contribute to the energy redistribution of electrons, which can be expressed as an electrical heating effect. The effect of electric field in this model is to increase the temperature of electrons, so that the temperature (T) is replaced by $T_{\text{eff}}=T+T_{\text{elec}}$, where $T_{\text{elec}}\sim eE\xi$. Hence, the temperature dependence of resistivity at different electric field can be rewritten as

$$\rho(T)=\rho_0 \exp\left(\frac{T_m}{T+T_{\text{elec}}}\right)^m=\rho_0 \exp\left(\frac{T_m}{T+eE\xi}\right)^m. \tag{4}$$

In the present case, we find that both the temperature and electric-field dependence of resistivity can be described best by the hot electron model. The $\rho(T)$ curves measured at different electric fields overlap each other quite well in the high-temperature range with a single $T_{1/4}$ value of 9000 K, as shown in Fig. 4(a). T_{elec} values increase with the electric field as expected [see the inset of Fig. 4(a)], and from the linear dependence of T_{elec} on electric field, the localization length is estimated to be about 260 Å. In CNT composites, the density of states (DOS) can be described as $n(E_F)=n_0(E_F)\times f$, where $n_0(E_F)$ is the DOS for SWNT and f is the volume fraction of the composite. Since the volume fraction is identical for the samples in this work, the change of slope in $\ln\rho$ versus $T_{\text{eff}}^{1/4}$ originates from the change of the localization length ξ. From the slope change of Fig. 4(b), we find that the localization length increased by about 20% for

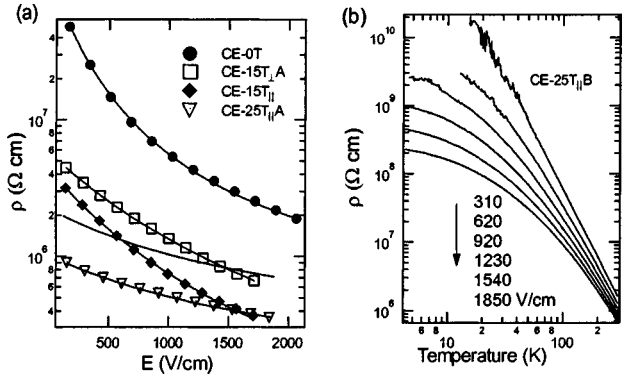

FIG. 3. (a) The room-temperature resistivity as a function of the electric field for various nanotube–epoxy composites. The fits are obtained from the Mott-type VRH conduction model with hot electron effect considered. (b) Electrical resistivity of CE-25T$_{\parallel}$B as a function of temperature at different electrical fields 310, 620, 920, 1230, 1540, and 1850 V/cm from the top curve downward.

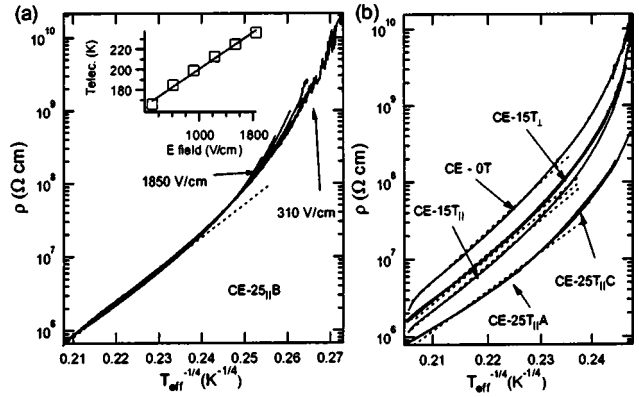

FIG. 4. $\ln \rho$ vs $T_{\text{eff}}^{-1/4}$ plot at high temperatures. (a) The data of Fig. 3(b) for sample CE-25$_{\|}$B for different electric fields. Inset: Relationship of T_{elec} to electric field [from Eq. (4)]. (b) The data for different samples from Fig. 2 for low electric fields.

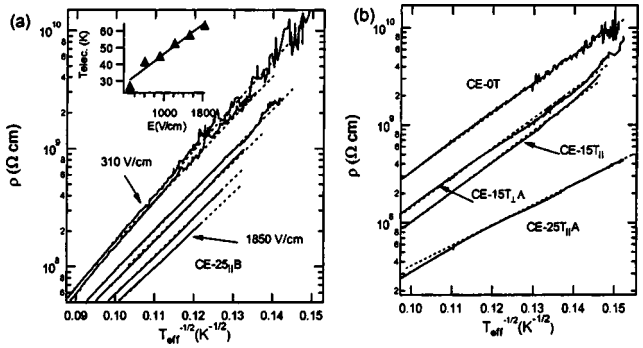

FIG. 5. $\ln \rho$ vs $T_{\text{eff}}^{-1/2}$ plot at low temperatures. (a) The data of Fig. 4(b) for sample CE-25$_{\|}$B for different electric fields. Inset: Relationship of T_{elec} to electric field [from Eq. (4)]. (b) The data for different samples from Fig. 2 for low electric fields.

the CE-25T$_{\|}$ compared to CE-0T. The values of $T_{1/4}$ and corresponding $\xi_{\text{ratio}}(\xi/\xi(\text{CE-0T}))$ derived from the high-temperature data are listed in Table I.

In Fig. 5, we examine the low-temperature behavior of the electrical transport, since the linear behavior in the $\ln \rho$ versus $T_{\text{eff}}^{1/4}$ plot clearly deviates at low temperatures, as observed in both Figs. 4(a) and 4(b). The crossover from Mott- to Efros-type VRH conduction is often observed in doped semiconductors, and is attributed to the existence of a soft Coulomb gap due to Coulomb correlations.[18,20] When the Coulomb gap is the same order of magnitude with the measured temperature range, Efros VRH cannot be seen at higher temperatures where thermal effects shadow the Coulomb gap. At lower temperatures, the Coulomb gap behavior emerges as a linear relation in the $\ln \rho$ versus $T^{1/2}$ plot. Since the hot electron model is still valid in the Efros VRH conduction regime, the $\ln \rho$ versus $T_{\text{eff}}^{1/2}$ plot of Fig. 5 supports the Efros VRH conduction model at low temperatures for our samples. The localization length ratio and the Coulomb gap derived from the Efros VRH model in the low-temperature region are also listed in Table I.

The existence of Coulomb correlation has also been observed in SWNT/[poly(methymethacrylate)] PMMA composites, where a smaller Coulomb gap (0.5–2.5 meV depending on the SWNT volume fraction) was reported.[10] It was argued that the Coulomb gap is due to the Coulomb charging energy involved in the transport process between bundles (or tubes). For an individual CNT bundle, the Coulomb charging energy was estimated to be about 2–7 meV from Coulomb blockade experiments.[21,22]

TABLE I. The summary of Mott and Efros VRH fitting results. ξ_{ratio} denotes the localization length ratio compared to the value of the nonaligned SWNT–epoxy composites [ξ/ξ(CE-0T)].

Samples	3D VRH (high T) $T_{1/4}$ (K)	ξ_{ratio}	Efros VRH (low T) $T_{1/2}$ (K)	Nonlinear R (295 K) ξ_{ratio}	$T_{1/4}$ (K)	ξ_{ratio}	Coulomb gap (meV)
CE-0T	14 030	1.00	1060	1.00	7270	1.00	25
CE-15T$_{\perp}$A	13 360	1.02	1220	0.95	7650	0.98	32
CE-15T$_{\perp}$B	12 696	1.03					
CE-15T$_{\|}$	13 190	1.02	1210	0.96	7560	0.99	32
CE-25T$_{\|}$A	10 950	1.09	700	1.15	2900	1.36	15
CE-25T$_{\|}$B	9000	1.16	650	1.18	3417	1.29	15
CE-25T$_{\|}$C	6600	1.29					

B. Thermal conductivity

The final area of our experimental investigation concerns thermal transport. The temperature dependence of thermal conductivity for the composite materials (CE-0T, CE-25T$_{\|}$) and control epoxy (E-25T) is shown in Fig. 6. Even without magnetic field processing, the thermal conductivity increases by up to 300% with 3 wt % SWNT loading. The thermal conductivity is further enhanced by magnetic processing, i.e., the thermal conductivity increases by another 10% by magnetic alignment in 25 T. The idea of increasing thermal conductivity by adding highly thermal conducting inclusions has been developed and practiced in many areas. If one considers an effective thermal conductivity K_{eff} for the inclusion of a randomly oriented elliptical material,[23] K_{eff} for the nonaligned sample (CE-0T) would be estimated to be about 33 W/mK, where we have assumed isolated SWNTs with a 2 nm diameter, 500 nm length, and $K \sim 3000$ W/mK thermal conductivity. Since the thermal conductivity of nonaligned

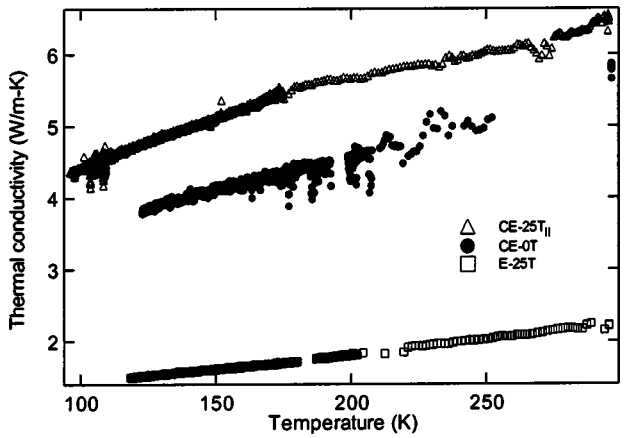

FIG. 6. Thermal conductivity of CNT–epoxy composites magnetically processed at 0 and 25 T, compared with the neat epoxy control sample (also processed at 25 T). The thermal gradient was applied along the magnetic field alignment direction.

nanotube–epoxy composite is 1/5 of the theoretical estimation, it is apparent that other effects that suppress the effective thermal conductivity should be considered.

IV. DISCUSSION

The results of our investigation are summarized by first considering the parameters that result from the electrical transport studies, as shown in Table I. (For the CE-15T$_\perp$B and CE-25T$_\parallel$C samples, only the high-temperature, 3D, VRH model results were determined.) The most apparent trends, for the magnetically processed SWNT–epoxy systems examined, are that the localization length is increased, and the Coulomb gap is decreased, if one compares the most aligned sample (CE-25T$_\parallel$) with the nonaligned sample (CE-0T). The absolute value of localization length is uncertain since the DOS of SWNTs $[n_0(E_F)]$ and the volume fraction (f) are not exactly known. However, if we assume the DOS of metallic SWNTs and 3% volume fraction,[24] the localization length for CE-0T is about 122 Å (Mott VRH), 74 Å (Efros VRH), and 152 Å (electric-field dependence) at room temperature. For the CE-25T$_\parallel$B sample, the localization lengths are about 142 Å, 120 Å, and 196 Å, derived from the same methods (respectively). Usually, the localization length derived from the electric-field dependence fit was larger (see also $\xi \sim 260$ Å derived from the electric-field dependence of T_{elec}), which may be explained by the moderate anisotropic VRH conduction.[25] In reference to Fig. 1, the average size of the localization length derived from our measurements (of order 100 Å) is in reasonable agreement with the corresponding size of the bundles observed in the AFM measurements.

The localization length values for CE-0T are similar in value to SWNT/PMMA composites, where volume fraction independent localization lengths were observed.[10] In the analysis of Ref. 10, the localization was assumed to be intrinsic, occurring at the bundle boundaries (transverse localization). The localization length derived in our work is also larger than the nanotube diameters, which indicates that the localization also occurs on bundle length scales. *Hence, the increase of the localization length in the aligned composite compared to that of the nonaligned one can be attributed to the increase of bundle size for the magnetically aligned nanotubes*. The decrease of the Coulomb gap in the aligned sample can be also explained in this context, since the Coulomb charging energy for larger bundles becomes smaller.[10] The enhanced bundling in the aligned sample may be attributed to the increase of van der Waals force between aligned individual nanotubes. Since the van der Waals force is strongly dependent on the distance between nanotubes, a small reorientation of nanotubes to the aligned direction could increase the van der Waals force resulting in bundling.

In addition to the bundling effect, the alignment of nanotubes in composites also seems to affect the electrical conductivity in terms of a temperature independent enhancement of electrical conductivity. This effect can be explained by the more efficient percolation path for the parallel direction and/or the decrease of disorder by alignment of nanotubes. The decrease of resistivity by a magnetic process and the weak temperature dependent anisotropy between CE-15T$_\perp$ and CE-15T$_\parallel$ can be also explained by this effect.

The increase in the thermal conductivity of epoxy (with the addition of a SWNT and magnetic field processing) is less pronounced than the increase in the electrical conductivity in the materials we investigated. It is known that the high thermal conductivity of CNTs comes from the large mean-free path of phonon transport. Since the phonon mismatch at boundaries of the nanotube and epoxy matrix results in high thermal boundary resistance (Kapitza resistance), the effective thermal conductivity should be substantially less than when Kapitza resistance was ignored. Furthermore, the phonon mode of CNTs can be affected by surrounding epoxy matrix as a strain, as observed in a shift of Raman modes (of order 5 cm^{-1}) in MWNT–PMMA composites,[26] and in the materials investigated herein (SWNT epoxy).[27] It is known that the ballistic thermal conductivity of an isolated CNT can be suppressed by intertube interactions in bundles. Therefore, if the magnetic alignment encourages bundling as the electrical conductivity data suggest, the effective thermal conductivity may be smaller than the value derived from the effect of the colinearity of the phonon wave vector exclusively. In fact, in magnetically aligned CNT mat samples, the thermal conductivity is five to eight times larger for the parallel direction compared to the perpendicular direction,[4,5] where, in the composites, we saw only a 10% increase of thermal conductivity with alignment.

V. CONCLUSIONS

We have observed the enhancement of electrical and thermal conductivities of CNT–epoxy composites with magnetic field processing. The cooperative alignment of nanotubes in the host–polymer system is identified as the main cause for the enhancement of the electric and thermal conductivities. Additional bundling of the SWNT appears to be promoted by magnetic processing, based on the electrical transport analysis. Although this may be advantageous for enhancing the electrical conductivity, bundling works against significant enhancements in the thermal conductivity. Therefore, it is desirable to find a route to make an aligned CNT composites with a higher degree of nanotube separation.

ACKNOWLEDGMENTS

Research at Florida State is supported by the NSF (Grant No. DMR 0203532), DARPA-DSO (MDA972-02-1-0017), and DOD (Grant No. DAAD19-01-1-0742). The NHMFL is supported by a contractual agreement between the NSF and the State of Florida.

[1] M. J. Biercuk, M. C. Llaguno, M. Radosavljevic, J. K. Hyun, A. T. Johnson, and J. E. Fischer, Appl. Phys. Lett. **80**, 2767 (2002).
[2] P. Kim, L. Shi, A. Majumdar, and P. L. McEuen, Phys. Rev. Lett. **87**, 215502 (2001).
[3] J. Hone, M. Whitney, C. Piskoti, and A. Zettl, Phys. Rev. B **59**, R2514 (1999).
[4] J. Hone, M. C. Llaguno, N. M. Nemes, A. T. Johnson, D. A. Walters, M. J. Casavant, J. Schmidt, and R. E. Smalley, Appl. Phys. Lett. **77**, 666 (2000).
[5] J. E. Fischer, W. Zhou, J. Vavro, M. C. Llaguno, C. Guthy, R. Haggenmueller, M. J. Casavant, D. E. Walters, and R. E. Smalley, J. Appl. Phys. **93**, 2157 (2003).

[6] A. L. Efros (unpublished).
[7] J. P. Lu, Phys. Rev. Lett. **74**, 1123 (1995).
[8] D. A. Walters, M. J. Casavant, X. C. Qin, C. B. Huffman, P. J. Boul, L. M. Ericson, E. H. Haroz, M. J. O'Connell, K. Smith, D. T. Colbert, and R. E. Smalley, Chem. Phys. Lett. **338**, 14 (2001).
[9] T. Kimura, H. Ago, M. Tobita, S. Ohshima, M. Kyotani, and M. Yumura, Adv. Mater. (Weinheim, Ger.) **14**, 1380 (2002).
[10] J. M. Benoit, B. Corraze, and O. Chauvet, Phys. Rev. B **65**, R241405 (2002).
[11] Carbon Nanotechnologies, Inc., 16200 Park Row, Houston, TX 77084.
[12] PTM&W Industries, Inc., 10640 S Painter Ave, Santa Fe Springs, CA 90670.
[13] H. Garmestani *et al.* (unpublished).
[14] R. Gaal, J. P. Salvetat, and L. Forro, Phys. Rev. B **61**, 7320 (2000).
[15] Y. Yosida and I. Oguro, J. Appl. Phys. **86**, 999 (1999).
[16] M. S. Fuhrer, W. Holmes, P. L. Richards, P. Delaney, S. G. Louie, and A. Zettl, Synth. Met. **103**, 2529 (1999).
[17] N. F. Mott and E. A. Davis, *Electronic Processes in Non-Crystalline Materials*, 2nd ed. (Oxford University Press, London, 1979).
[18] B. I. Shklovskii and A. L. Efros, *Electronic Properties of Doped Semiconductors* (Springer, Berlin, 1984).
[19] J. Zhang, W. Cui, M. Juda, D. McCammon, R. L. Kelley, S. H. Moseley, C. K. Stahle, and A. E. Szymkowiak, Phys. Rev. B **57**, 4472 (1998).
[20] H. S. Moreira, J. F. Sampaio, E. S. Alves, and A. G. de Oliveira, Phys. Rev. Lett. **80**, 1706 (1998) and references therein.
[21] M. Bockrath, D. H. Cobden, J. Lu, A. G. Rinzler, R. E. Smalley, L. Balents, and P. L. McEuen, Nature (London) **397**, 598 (1999).
[22] M. Bockrath, D. H. Cobden, P. L. McEuen, N. G. Chopra, A. Zettl, A. Thess, and R. E. Smalley, Science **275**, 1922 (1997).
[23] T. Miloh and Y. Benveniste, J. Appl. Phys. **63**, 789 (1988).
[24] The specific gravity of the epoxy is 1.1, which is comparable to SWNTs.
[25] A. A. Maarouf, C. L. Kane, and E. J. Mele, Phys. Rev. B **61**, 11156 (2000).
[26] C. Stephan, T. P. Nguyen, B. Lahr, W. Blau, S. Lefrant, and O. Chauvet, J. Mater. Res. **17**, 396 (2002).
[27] D. L. Eaton (unpublished).